Int. J. Electrochem. Sci., 11 **(2016)** 10256 – 10269, doi: 10.20964/2016.12.29

International Journal of ELECTROCHEMICAL SCIENCE
www.electrochemsci.org

Novel Magnetic Nanocomposites Comprising Reduced Graphene Oxide/Fe_3O_4/Gelatin Utilized in Ultrasensitive Non-Enzymatic Biosensing

Seyed Morteza Naghib[1*], *Mehdi Rahmanian*[2*], *Keivan Majidzadeh-A*[2,3*], *Sasan Asiaei*[4,5], *Omid Vahidi*[4,6],

[1] Nanobioengineering Division, Nanotechnology Department, School of New Technologies, Iran University of Science and Technology (IUST), P.O. Box 16846-13114, Tehran, Iran.
[2] Breast Cancer Research Center (BCRC), Academic Center for Education, Culture and Research (ACECR), Tehran, Iran.
[4] Sensors and Intergrated Bio-Microfluidics/MEMS lab (SIBlab), Iran University of Science and Technology (IUST), P.O. Box 16846-13114, Tehran, Iran.
[5] School of Mechanical Engineering, Iran University of Science and Technology (IUST), P.O. Box 16846-13114, Tehran, Iran.
[6] School of Chemical Engineering, Iran University of Science and Technology (IUST), P.O. Box 16846-13114, Tehran, Iran.
[*]E-mail: mrahmanian1@gmail.com, kmajidzadeh@razi.tums.ac.ir, naghib@iust.ac.ir,

Received: 23 May 2016 / *Accepted:* 2 August 2016 / *Published:* 10 November 2016

Measuring the concentration of glucose is important to prevent the growth of cancer cells. Electrochemical enzyme based biosensors offer highly selective and sensitive detection of glucose at the expense of limited stability. Therefore, development of simple, sensitive, fast and reliable devices has a great importance for the determination of glucose level. In this paper, reduced graphene oxide (rGO)-Fe_3O_4-gelatin amended glassy carbon electrode (GCE) was used as an advanced magnetic nanobiosensor for non-enzymatic determination of glucose concentration. The nanocomposite, rGO-Fe_3O_4-gelatin, has been firmly coated on GCE, developed by a relatively simple technique. The resulting cyclic voltammograms exhibited a pair of well defined, irreversible and stable peak for redox systems, acquired in buffer solution. The developed biosensor demonstrated an excellent catalytic activity towards the oxidation of glucose at a positive potential in buffer solution, which is relatively unusual. This novel nanosensor also exhibited high sensitivity, enhanced shelf-life (> 2 month), wide linear range (0.1-10 mM) and low detection limit (0.024 µM). To the best of our knowledge, the aforementioned electroanalytical characteristics of this nonenzymatic biosensor are superior to previously reported modifications of nonenzymatic glucose biosensors.

Keywords: Nonenzyme electrode, Glucose sensing, Cyclic voltametry, Gelatin, Stability, Selectivity.

1. INTRODUCTION

Biomarkers overexpressed on the tumor cells facilitate high rates of glucose catabolism and cause tumor cell proliferation [1]. Therefore, measuring the concentration of blood glucose level is critical for patient diet. Immobilized enzymes have been used in developing novel analytical and sensing elements, and there are a number of reports on advancing their surface activity, functionality, and morphology. These developments in conjunction with advanced materials have deepened our understanding from bioreceptors immobilization, catalytic activity of the immobilized bioreceptors, and their superior properties [2-5]. The resulting biosensors allow promising developments for medical diagnosis, due to their convenient process ability, cost effectiveness and excellent selectivity [6-9]. The first successfully commercialized biosensors for diabetes mellitus are based on electrochemical techniques [10-12]. Glucose oxidase (GOD) has been widely used as the main biological element for glucose sensing. Although electrochemical GOD based biosensors offer selective and sensitive detection of glucose, the stability of GOD biosensors is very low [11, 12]. Therefore, development of a simple, sensitive, fast and reliable glucose sensing device has a great importance, yet to be tackled.

Graphene nanomaterials have exhibited promises for recent biosensing demands due to their superior catalytic properties [12-16]. Graphene is inherently a zero-gap semiconductor with exceptionally high electron mobility in ambient condition, even higher than carbon nanotubes [17, 18]. Graphene oxide (rGO), a member of graphene nanomaterial family, is one of the best nanomaterials for fabrication of electrochemical sensors due to a number of exceptional properties including: catalytic properties [16, 19], unusually large specific surface area (two accessible sides), excellent water solubility and a great amount of oxygen containing surface functionalities, comprising epoxide, hydroxyl, and carboxylic acid groups [12, 13, 20]. The intrinsic oxygen-containing functional groups have been used as initial sites for deposition of metal nanoparticles on the rGO sheets, which open up a novel route to multifunctional nanometer scaled catalytic, electronic, and magnetic materials [21].

Magnetite incorporated nanomaterials demonstrate the same effects as conductive nanoparticles and also provide additional ferromagnetic effects [5]. Use of external magnetic fields for preparation of nanomaterials allows easy manipulation of the nanomaterials, e.g. in separation and cleaning processes, coating on electrode surface, etc.[22]. Magnetic nanomaterials are interesting for many researchers due to their wide application in magnetic resonance imaging, drug delivery, biological separation, catalysis, and biosensing[23, 24]. The catalytic properties of magnetic nanomaterials are dependent on their morphology, structure and size. Different sizes of Fe_3O_4 have been investigated and the smallest reported size of Fe_3O_4 (30 nm) exhibits an excellent catalytic activity [25]. This event is due to the exceptionally high surface-to-volume ratio of the nanoparticles and its small size which assures appropriate interaction with substrates.

Gelatin, as a natural protein polymer, has been widely utilized to immobilize catalytic enzymes and other biological elements [26, 27]. Immobilization of enzymes and other bio-receptors such as antibodies or aptamers, on gelatin biopolymers can be achieved by covalent cross-linking of the amino groups of gelatin and the enzyme molecule. The cost benefit and availability of this biopolymer is superior to other competitors, such as chitosan, polyacrylamide, polymethylmeta acrylate (PMMA), and algenic acid [26].

In this paper, we have developed a nonenzymatic biosensor for glucose detection at the continuation of our studies on detection of biomolecules [8, 9, 20, 28-30], preparation Magnetic rGO (Fe_3O_4-rGO) is used for the electrochemical oxidation of glucose at magnetic nanomaterials modified glassy carbon electrode (GCE) and developing a new nonenzymatic electroanalytical procedure to the determination of the analyte.

2. MATERIALS AND METHODS

2.1. Reagent

All chemicals were acquired in analytical grade from Merck (Darmstadt, Germany) were used without further purification. All solutions were prepared with doubly distilled water. Electrochemical measurements were carried out in a conventional three-electrode cell powered by an electrochemical system comprising an AUTOLAB system with PGSTAT302N boards (Eco Chemie, Utrecht, Netherlands). The system operated on a PC using Nova 1.7 software. An Ag/AgCl electrode was used as the reference electrode. All potentials were measured with respect to the Ag/AgCl, which was positioned as close to the working electrode as possible by means of a Luggin capillary. Buffer solutions (0.1 M) were prepared from phosphoric acid (H_3PO_4) and disodium hydrogen phosphate (Na_2HPO_4). The solutions were deoxygenated by bubbling high purity (99.99%) argon gas through them, prior to the experiments. All the electroanalytical tests were carried out at 25 °C in 0.1 M PBS.

2.2. Synthesis of Fe_3O_4-rGO

rGO was prepared by chemical oxidization of graphite powder according to the modified Hummers method [19]. Briefly, 1 g graphite was placed in 50 mL H_2SO_4 under stirring condition (600 rpm). Next, the solution was placed in cold area (10 min) and consequently 6 g $KMnO_4$ was leisurely sprayed into it. Eventually, 200 mL deionized water and 6 mL H_2O_2 (30%) was added to reduce residual permanganate. The residual salts and acids of the graphite oxide suspension were removed by centrifugation at 8000 rpm for 90 min. The graphite oxide was interspersed in deionized water to take an aqueous graphite oxide suspension with yellow-brownish color. The graphite oxide suspension (20 mL) was put on the glassy carbon electrode and allowed to dry in air, and then 10 mL 0.05 wt% Nafion was cast on the electrode and allowed to dry in air. The electrochemical reduction of graphite oxide was performed with cyclic voltammetry (-1 v to +1 v at a scan rate of 50 $mV.s^{-1}$) in 0.1 M Na_2SO_4 solution in a standard three-electrode cell. Fe_3O_4-rGO were synthesized by co-precipitation of $FeCl_3 \cdot 6H_2O$ and $FeCl_2 \cdot 4H_2O$, in the presence of rGO [4]. An aqueous solution of ferric chloride and ferrous chloride was prepared in a 2:1 mole ratio. For the preparation of Fe_3O_4-rGO, 40 mg of rGO in 40 mL of water was sonicated for 30 min, and then 50 mL solution of $FeCl_3$ (110 mg), $FeCl_2$ (43 mg) and 20 mL 30% ammonia solution in deionized water were added at room temperature.

2.3. Preparation of Fe_3O_4-rGO-gelatin

Gelatin (1.5 g) was dissolved in 50 ml of 50 mM Tris acetate buffer (pH 7.3) by heating at 60°C with continuous stirring for 1 h to obtain a clear solution. This solution was cooled and the solidified mixture was stored at 4°C. Prior to final modification, the mixture was heated to 60 °C and then slowly brought to 27°C to obtain a clear solution [26]. A clear solution of gelatin (30 mg/ml), 25 % (v/v) Fe_3O_4-rGO and 0.1 % (v/v) glutaraldehyde were mixed together and stirred for 10 s (400 rpm). Afterward, the mixture was cast in hollow plastic cylinders (0.5 cm×0.5 cm) and kept at 4°C for 24 h to purify the composite. Finally, the mixture was electrodeposited on the electrode. Figure 1 below illustrates the procedure of sensing electrode preparation:

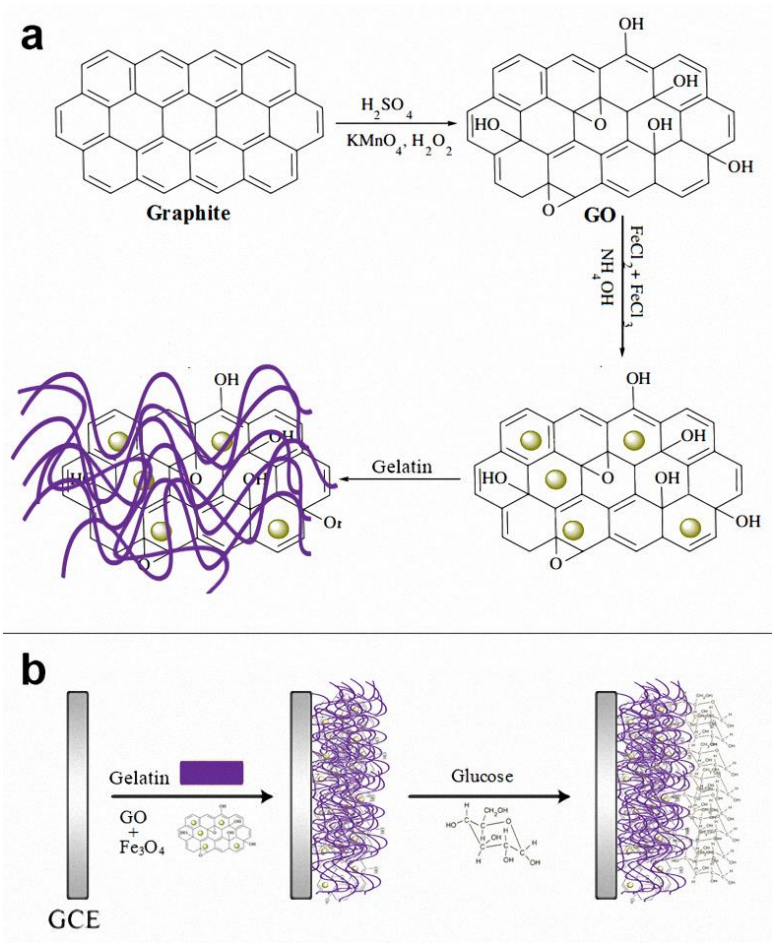

Figure 1. Schematic representation of the process flow for preparation of the nanocomposite on the sensing electrode.

3. RESULTS AND DISCUSSION

3.1. Electrodeposition of nanocomposite

Electrodeposition properties of the developed nanocomposite on the glassy carbon electrode (GCE) is described by depicting it cyclic voltammograms in figure 2 below (Number of scan = 30).

The cyclic voltammogram are drawn in a potential range of 0.0 to -1.5 V and indicated a large cathodic current peak at -0.81 V with a starting potential of -0.5 V. This large reduction current is due to the reduction of the surface oxygen groups, since water, the other competitor, is reduced to hydrogen at more negative potentials (e.g., -1.5 V or lower). In the second cycle, the reduction current (at negative potentials) decreased significantly and disappeared after several potential scans. This indicates a rapid and irreversible reduction of surface-oxygenated components on exfoliated rGO which occurs electrochemically at negative potentials.

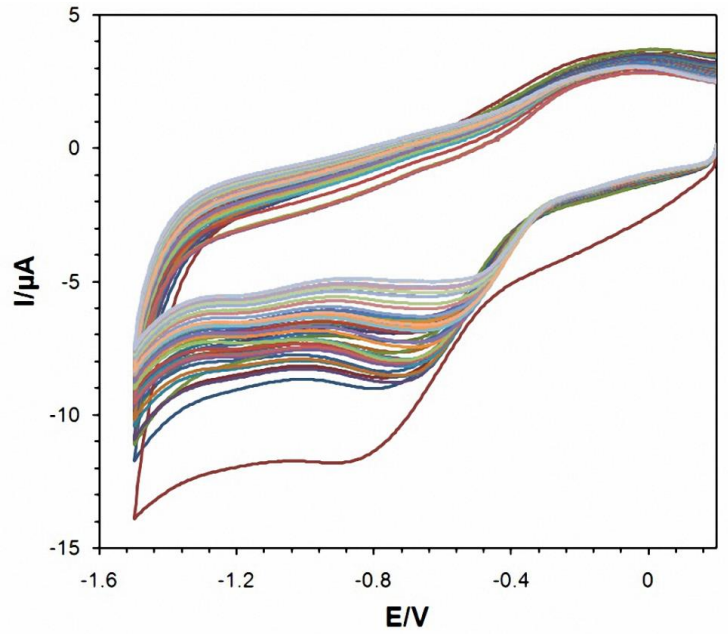

Figure 2. Cyclic voltammograms of a nanocomposite modified GCE in PBS (pH 7.4) at a scan rate of 30 mV/s (Number of scan = 30).

3.2. Effect of pH on Current Response of the Enzyme Electrode

pH has a significant influence on the activity of glucose biosensors. We studied the impact of pH by recording the response changes under different values of pH at the ambient temperature, 25 °C. Figure 3a indicates cyclic vlotammograms (CVs) of the nanocomposite modified electrode measured in the 100 mM PBS buffer at various pH values with introduction of a 200 μM glucose sample. The scan rate was set at 30 mV/s and pH was adjusted by addition of appropriate amount of 1 mM NaOH and 1 mM HCl solutions.

Figure 3b shows output current of the biosensor at various pH values. As depicted in figure 3b, the electrode exhibited low activity on pH < 6 and high activity on pH > 6. This observation has great practical implications due to the fact that most of the biological samples have pH values of greater than 6. Therefore, the majority of biological fluids can be analyzed with optimum sensing activity with this novel nanocomposite. To benefit from an enhanced sensing activity, all subsequent electrochemical experiments were carried out in 0.1 M PBS buffer solution at pH 7.4.

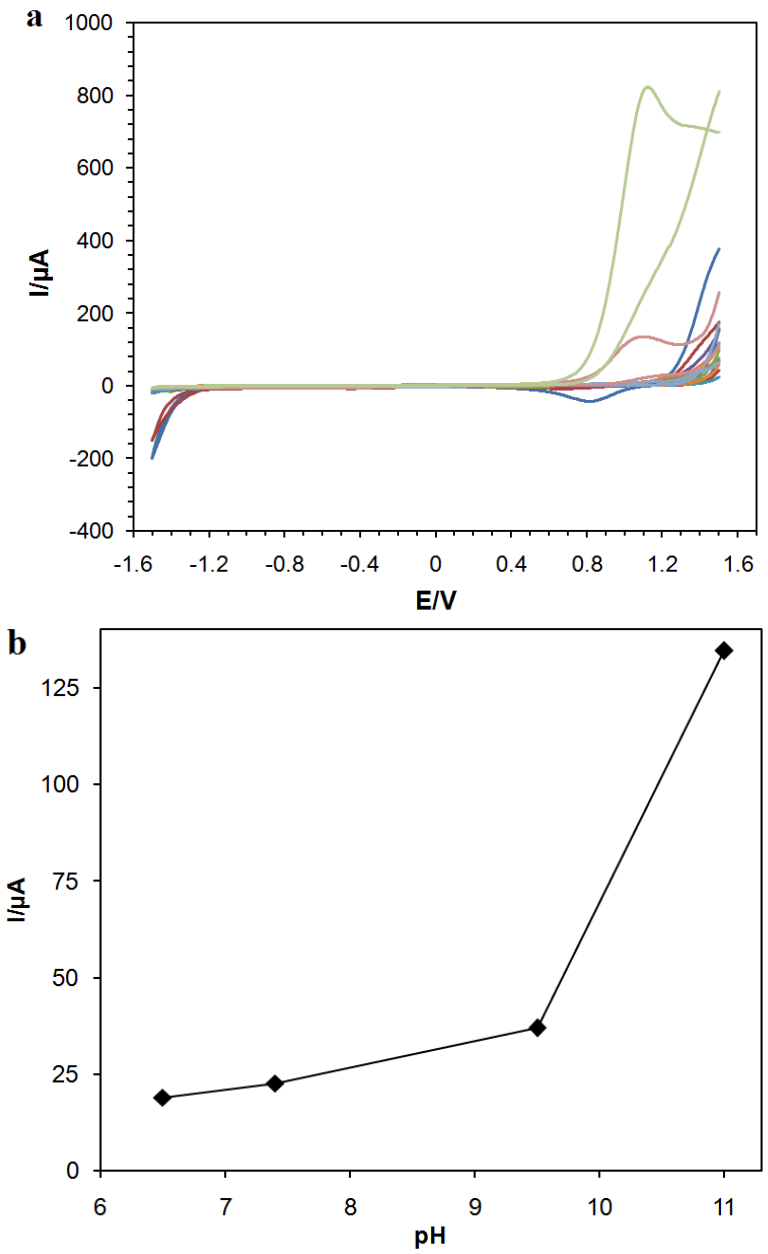

Figure 3. a) CVs responses of the nanocomposite modified electrode in different pHs; b) Output current of the biosensor at various pH values. Initial working volume is 10 mL PBS buffer 100 mM containing 200 µM glucose solution.

3.3. The Linear Response and Diffusion Behavior of the modified surface

Figure 4a shows cyclic voltammograms for Fe_3O_4-rGO-gelatin in the PBS buffer solution (pH = 7.4) at different scan rates. In Fig. 4-B, the anodic and cathodic peak currents are directly proportional to the scan rate from 10 to 150 $mV \times s^{-1}$. The plot of peak current versus the scan rate up to 10 $mV \times s^{-1}$ exhibits a nearly linear relationship (figure 4b). This phenomenon is expected for the surface confined redox processes and confirms catalytic properties for our novel biosensing device. The small peak-to-peak separation and proper linearity between the peak currents and the sweep scan

rates of 10–150 $mV \times s^{-1}$ implies facile charge transfer kinetics through the nanocomposite. At higher scan rates, the currents' peak versus the scan rate deviates from linearity and the currents' peak became directly proportional to the potential scan rate square root. Presumably, at the higher bound of scan rates, the current peak is limited by the diffusion process. Moreover, with further increase of the scan rate, the peak separations begins, implying limitations in the charge transfer kinetics.

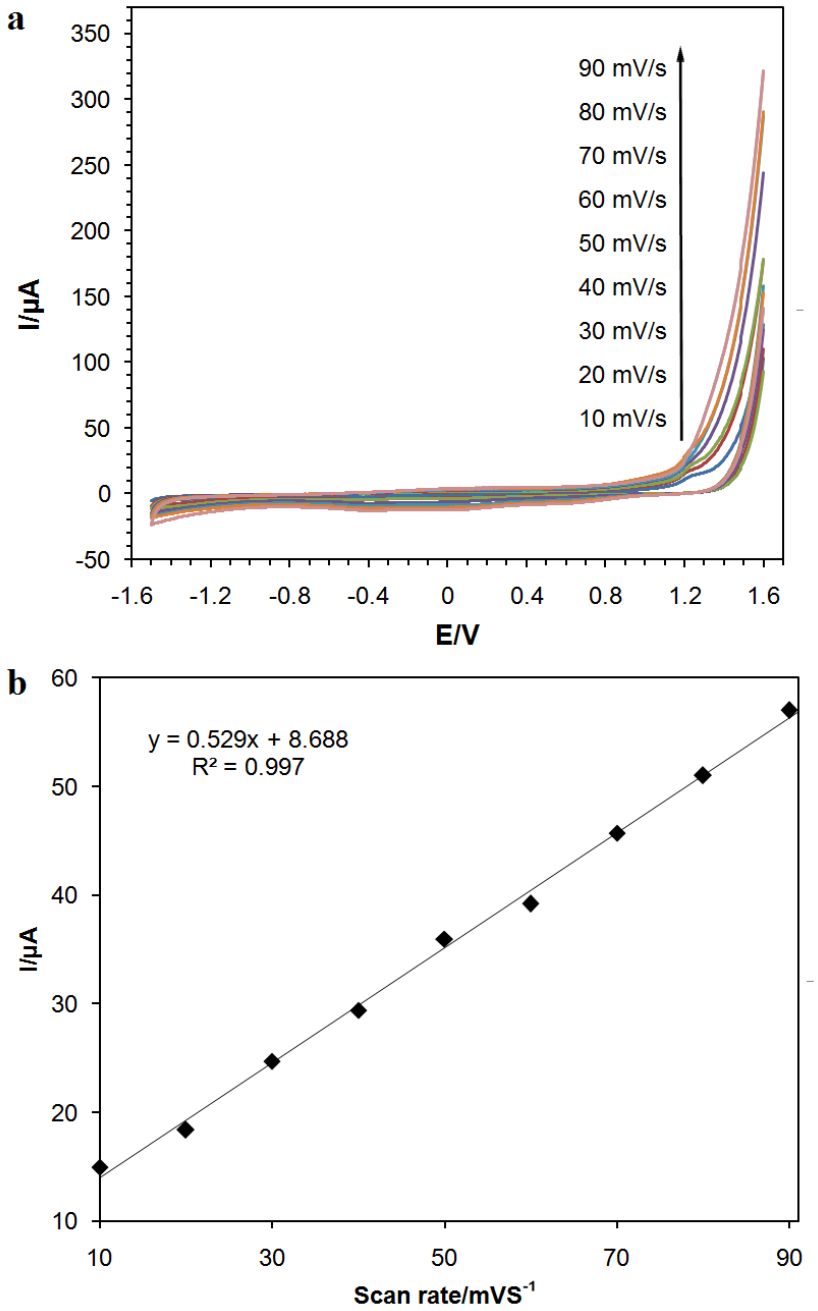

Figure 4. a) Cyclic voltammetry curves of the Fe_3O_4-rGO-gelatin in the buffer solution (pH = 7.4) at scan rates (inner to outer) 10, 20, 30, 40, 50, 60, 70, 80, 90 and 100 mV s^{-1}; b) Data points are connected by straight lines to aid visualization: a nearly linear relationship between the scan rate and peak current applies, confirming at the higher bound of scan rates, the current peak is limited by the diffusion process.

3.4. Glucose Sensing Process

The performance of the developed biosensor was evaluated by cyclic voltammetry (CV) technique, due to its simplicity and availability. The nanocomposite demonstrated comparable/superior properties to super conductive substrates and the functional groups on the GCE surface were highly sensitive for diagnosis of diabetes mellitus.

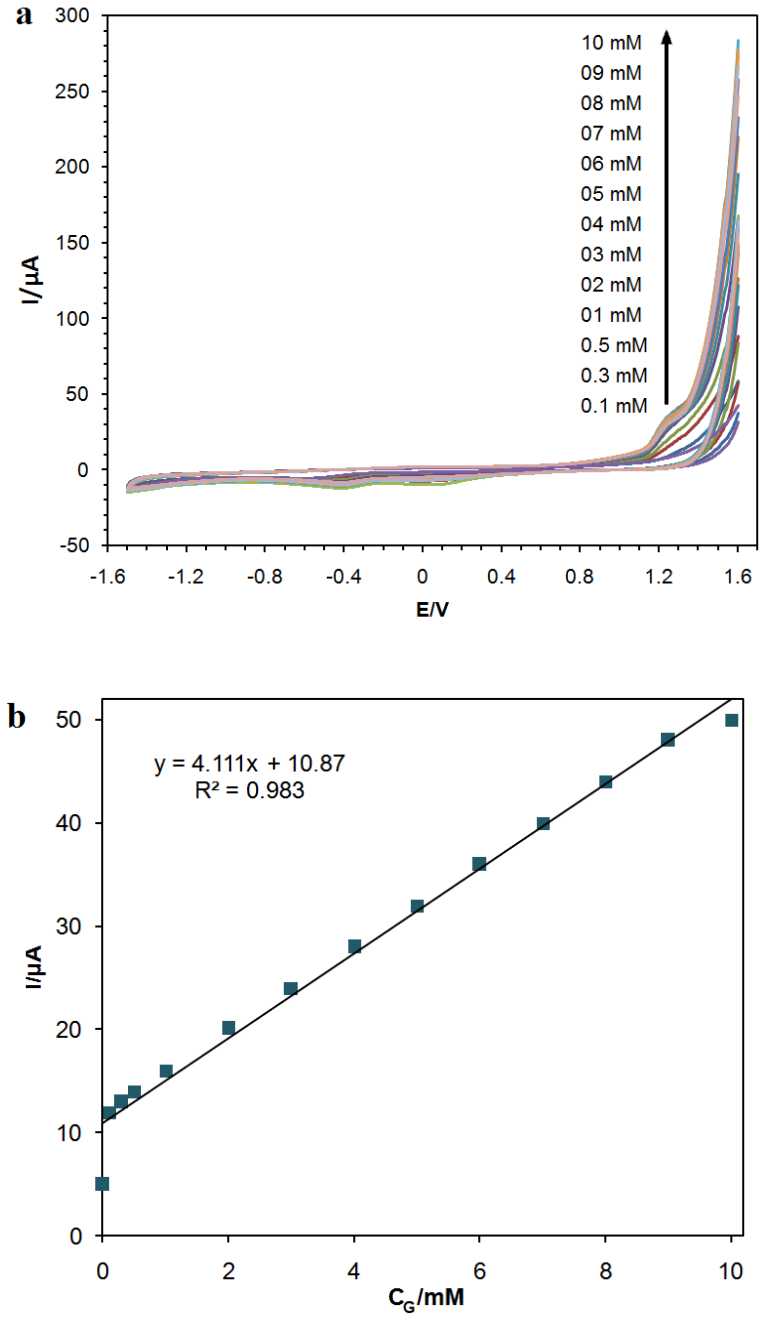

Figure 5. a) CVs of the nanocomposite modified electrode at scan rate of 30 mV/s for 0.1 to 10 mM of glucose concentrations; b) A linear response related to the analyte increasing in the range of 0.1 to 10 mM. Initial working volume: 10 mL; supporting electrode: 100 mM PBS buffer pH 7.4 (N=5).

The CV experiments of the nanocomposite modified electrode were accomplished in 100 mM PBS buffer (pH 7.4). The electrode surface was coated by electrodepositing the nanoparticles onto the surface of 10 GCE samples (Figure 1). The variations in particle size and average thickness among electrodes are expected to be negligible, since all the nanocomposite layers were electrodeposited under the same conditions. Therefore, the conductivity of the nanocomposite electrodeposited on each electrode surface is considered to be nearly equal. At any case, the conductivity measurements performed along the samples showed less that 5% of variation under same experimental conditions.

Figure 5a shows CV diagrams of the nanocomposite modified electrode in 0.1 M PBS buffer (pH 7.4) at a scan rate of 30 $mV \times s^{-1}$. Two peaks are obvious in all curves and accounts for non-enzymatic reactions or the reversible redox. In the oxidation current curves, a remarkable increase is observed at +1.15 mV vs. Ag/AgCl, indicating that the rGO-Fe_3O_4-gelatin deposited electrode provides favorable conditions for transferring electrons between the conductive substrate and the functional groups. The detection limit achieved was 0.024 μM (S/N = 3), and a nearly linear relationship between the peak current and the glucose concentration was observed for 0.1 to 10 mM samples in 0.1 M PBS, correlation factor is R^2= 0.983 (Figure 5b). The response of the biosensor to the substrate reduction increases linearly (nearly: R^2=0.983) with addition of the analyte to the buffer, within the desirable range, suitable for all glucose biosensing applications.

The sensitivity of the biosensor was calculated to be 2.3 × 10^{-3} A/(M.cm2), revealed by the CV experiments. Moozarm Nia et al. investigated electrodeposition of copper oxide/polypyrrole/reduced graphene oxide as a nonenzymatic glucose biosensor. The sensor depicted a sensing range of 0.1–10 mM (R2 = 0.991) of glucose and the detection limit reaches 0.03 M [31]. Lu et al. fabricated a graphene based nonenzymatic glucose biosensors by in situ synthesis of palladium nanoparticle–graphene nanohybrids. The sensor could be applied to the quantification of glucose with a wide linear range covering from 10 μM to 5 mM (R = 0.998) with a detection limit of 1.0 μM [32]. Luo et al. investigated on a non-enzymatic glucose sensor based on Cu nanoparticle modified graphene sheets electrode. The sensor presented a linear range up to 4.5 mM glucose with a detection limit of 0.5 M [33]. Nonenzymatic sensing of glucose using a carbon ceramic electrode modified with a composite film made from copper oxide, overoxidized polypyrrole and multi-walled carbon nanotubes was presented by Yu et al. The sensing range was from 20 μM to 10 mM, and the detection limit was 4.0 μM [34]. Cao et al. developed a non-enzymatic glucose sensor modified with Fe_2O_3 nanowire array. The sensing range and the detection limit of the sensor were 0.015–8 mM and 6.0 μM, respectively [35].

Based on table 1, the sensing range and detection limit of the developed biosensor (0.1–10 mM and 0.024 μM) are similar to or considerably greater than that of other graphene or magnetic based non-enzymatic biosensors for determination of glucose, making rGO-Fe_3O_4-gelatin high potential for clinical applications. The high sensitive catalytic performance, the wide linear range and low detection limit can be attributed to the nature of rGO based on gelatin matrix and moreover the existing rGO as a substrate for upper layer which increase the electron transfer and conductivity of the device. Comparing the rGO-Fe_3O_4-gelatin modified electrode and rGO-Fe_3O_4-modified electrode, it was found that due to the synergic effect of rGO-Fe_3O_4-gelatin, the latter has a wider linear detection range toward electrocatalytic oxidation of glucose. Furthermore, rGO particles can finely entrap the gelatin

and the rGO-Fe_3O_4 can highly raise the electrocatalytic active areas and enhance electron transfer. Additionally, the rGO-Fe_3O_4-gelatin nanocomposites can provide larger surface area for glucose molecules to be detected, adequately enhanced electrons. In addition, the linear sensing range of our biosensor, from 0.1 to 10 mM, is suitable for the clinical monitoring applications, provided that saliva glucose level is normally maintained higher than 0.3 mM. It seems the presence of semi-cross linked gelatin as a porous material caused novel sensory characteristics including desirable linear range, excellent sensitivity and lower detection limit than similar substrate. Moreover, the stability of the biosensor dramatically increased due to cross-linking the gelatin matrix on the surface (enhancing magnetic-based nanocomposite absorption on the electrode).

Table 1. Comparison of this work with other related publications.

Reference	Electrode	Detection limit	Linear range	Stability
This work	rGO-Fe_3O_4-gelatin	0.024 μM	0.1-10 mM	> 2 month
[31]	CuxO/Ppy/rGO	0.03 μM	0.1–10 mM	-
[32]	PdNPs/graphene	1 μM	0.01-5 mM	-
[33]	Cu/graphene	0.5 μM	up to 4.5 mM	-
[34]	CuO/OPpy/MWCNTs/CCE	0.05 μM	Up to 2 mM	-
[35]	Fe_2O_3 nanowire arrays	6 μM	0.015-8 mM	-
[36]	Sandwich-structured CuO	~1 μM	Up to 3.2 mM	-
[37]	CuxO/Ppy/Au	6.2 μM	Up to 8 mM	-
[38]	Porous Cu–NiO	0.5 μM	0.5–5 mM	-
[39]	NA/NiONF-rGO/GCE	0.77 μM	0.002–0.6 mM	-
[40]	Cu_2O/NiOx/rGO/GC	0.4 μM	0.87–2.95 mM	-
[41]	Porous CuO	0.14 μM	0.001–2.5 mM	-
[42]	NiO/carbon paste	0.16 μM	1–110 μM	-
[43]	Cu/CNTs	0.21 μM	0.007– 3.5 mM	-
[44]	Nanoporous Pt/Pb networks	-	1-16 mM	-
[45]	Co/Pc/ tetrasulfonate	0.1 mM	0.25–20 mM	-
[46]	Cu_2O/GNs	3.3 μM	0.3-3.3 mM	-
[47]	Cu_2O/Carbon Vulcan XC-72	2.4 μM	up to 6 mM	-
[48]	Pt/MWCNTs	-	1.0–26.5 mM	-
[49]	Cu_2O microcubes	0.8 μM	up to 500 μM	-
[50]	Ni hexacyanoferrate	1.25 μM	0.005-2.5 mM	-
[51]	FeOOH nanowire	7.8 μM	0.015-3 mM	-

3.5. Shelf Life, Selectivity and Reproducibility

The proposed biosensor has a great selectivity toward glucose, examined here by introduction of electroactive substances along with glucose and monitoring the current response of the biosensor, demonstrated in Figure 6. The existence of possible interference from other substances on glucose sensing, solutions containing 3.0 mM uric acid, ascorbic acid, lysine, arginine, histidine and cholesterol were prepared and introduced to the electrode along with glucose. The results indicates an

increase of 5.97% (max) and 2.42% (min) decrease in the current response of the biosensor, respectively (Figure 6). This observation confirms that the proposed glucose biosensor has a high selectivity toward glucose with no interference with other endogenously existing electroactive substances due to the nonenzymatic catalytic reaction.

The stability and reproducibility of the rGO-Fe_3O_4-gelatin modified GCE were examined by measuring the current response of the nanocomposite modified electrode upon introduction of 200 µM glucose. The average relative standard deviation (RSD) has always been below 5.12%. In a series of 10 sensors prepared under the same conditions, a RSD of 3.35% was obtained, indicating the reliability of the biosensor. In order to evaluate the stability of the sensor, the current response to 200 µM glucose was recorded every 4 days. It was found that the current could retain 90% of its original signal strength after 8 weeks of storage in room temperature, demonstrating the outstanding stability of the developed biosensor.

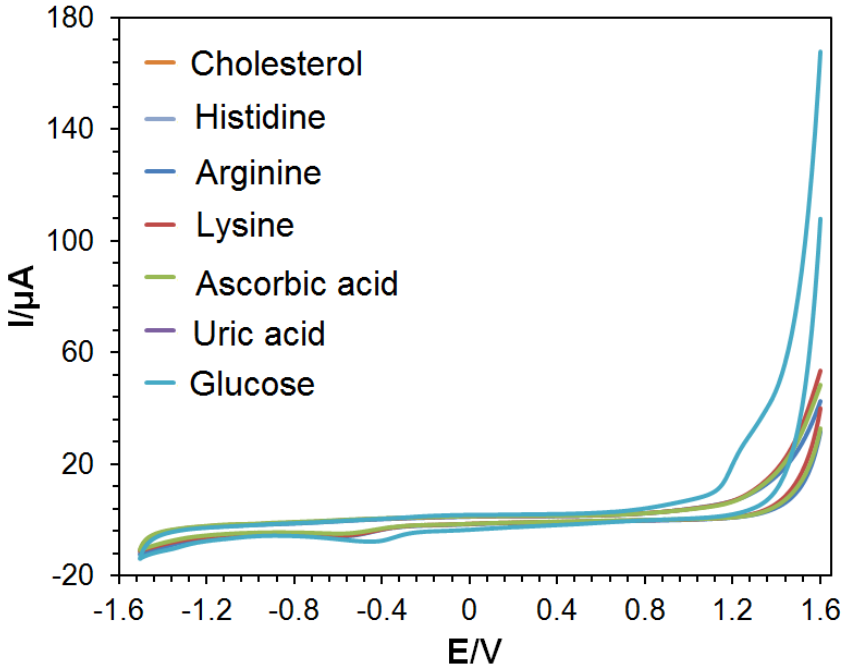

Figure 6. Selectivity evaluation of the nanocomposite based biosensor in presence of 3 mM uric acid, ascorbic acid, lysine, arginine, histidine and cholesterol. Initial working volume: 10 mL; supporting electrode: 100 mM PBS buffer pH 7.4 (N=5).

3.6. Real sample evaluation

Because of further certification, the potential of the optimized non-enzymatic biosensor for glucose monitoring in real sample was studied. The biosensor was applied to determination of the analyte level in human blood by a gold standard addition method. According to our knowledge the glucose normal range in human blood is 4.5 to 6.5 mM. The human blood samples offered by several humans were gifted from Tehran University of Medical Sciences. Ten real extractions (from different humans) with different glucose concentrations of 0.5, 1.0, 3.0, and 8.0 mM (evaluated with a gold standard method) were tested by the sensor. Based on the table 2, the recovery of the current responses

of the sensor is in the range of 98.5–109.17% and the relative standard deviation (RSD %) is in the range of 0.48-6.20%. These results demonstrated that the developed non-enzymatic sensor can be initially utilized to recognize diabetes mellitus in clinical diagnosis.

Table 2. Determine the glucose recovery results in the blood real samples by the non-enzyme sensor (N=5).

Real samples	The addition content	The detection content	RSD (%)	Recovery (%)
Human blood (200 μM)	0.0 mM	0.186 mM	5.13	-
	0.5 mM	0.724 mM	2.38	103.43
	1.0 mM	1.31 mM	6.20	109.17
	3.0 mM	3.152 mM	1.07	98.5
	8.0 mM	8.256 mM	0.48	100.68

4. CONCLUSION

We have demonstrated a nonenzymatic biosensor based on rGO-Fe_3O_4-gelatin fabricated by electrodeposition of a magnetic nanocomposite on the surface of GCE. The modified electrode demonstrated a high electrocatalytic activity for the glucose detection, superior to almost all previously reported competitors. The developed biosensor had a considerably low detection limit, high sensitivity, extraordinary stability in 2 months and a considerably wide linear range which is suitable for all clinical applications. This has all been due to the catalytic nature of Fe_3O_4 towards glucose, combined with the high surface area of rGO and gelatin matrix make a suitable nanocomposite and proposes a real promise for the development of future low cost nonenzymatic biosensors.

ACKNOWLEDGEMENT
This research was financially supported by Brest Cancer Research Center (BCRS) of Iran, and the Iran University of Science and Technology (IUST), Iran. The authors would like to acknowledge the products and services provided by IUST and BCRS that facilitated this research, including experimental setups.

References

1. A. Annibaldi and C. Widmann, *Curr Opin Clin Nutr Met Care*, 13 (2010) 466.
2. A. Bódalo, J.L. Gómez, E. Gómez, J. Bastida and M.F. Máximo, *Chemosphere*, 63 (2006) 626.
3. U.T. Bornscheuer, *Angew Chem Int Edit*, 42 (2003) 3336.
4. B. Chen, N. Pernodet, M.H. Rafailovich, A. Bakhtina and R.A. Gross, *Langmuir*, 24 (2008) 13457.
5. E. Omidinia, N. Shadjou and M. Hasanzadeh, *Mater Sci Eng C*, 33 (2013) 4624.
6. M. Hasanzadeh, N. Shadjou, M. Eskandani and M.d.l. Guardia, *TrAC-Trend Anal Chem*, 40 (2012) 106.
7. M. Hasanzadeh, N. Shadjou, E. Omidinia, M. Eskandani and M. de la Guardia, *TrAC-Trend Anal Chem*, 45 (2013) 93.
8. S.M. Naghib, M. Rabiee, E. Omidinia and P. Khoshkenar, *Electroanal,* 24 (2012) 407.
9. S.M. Naghib, M. Rabiee, E. Omidinia, P. Khoshkenar and D. Zeini, *Int. J. Electrochem. Sci*, 7 (2012) 120.

10. M. Hasanzadeh, N. Shadjou, M. de la Guardia, M. Eskandani and P. Sheikhzadeh, *TrAC-Trend Anal Chem*, 33 (2012) 117.
11. J. Wang, *Chem Rev*, 108 (2008) 814.
12. R. Wilson and A.P.F. Turner, *Biosens Bioelectron*, 7 (1992) 165.
13. Y. Wang, Z. Li, J. Wang, J. Li and Y. Lin, *Trend Biotechnol,* 29 (2011) 205.
14. T. Kuila, S. Bose, P. Khanra, A.K. Mishra, N.H. Kim and J.H. Lee, *Biosens Bioelectron*, 26 (2011) 4637.
15. Y. Liu, D. Yu, C. Zeng, Z. Miao and L. Dai, *Langmuir*, 26 (2010) 6158.
16. [Y. Shao, J. Wang, H. Wu, J. Liu, I.A. Aksay and Y. Lin, *Electroanal,* 22 (2010) 1027.
17. P.M. Ajayan, *Chem Rev*, 99 (1999) 1787.
18. A.K. Geim and K.S. Novoselov, *Nat Mater*, 6 (2007) 183.
19. V.C. Sanchez, A. Jachak, R.H. Hurt and A.B. Kane, *Chem Res Toxicology*, 25 (2012) 15.
20. S.M. Naghib, M. Rabiee and E. Omidinia, *Int. J. Electrochem. Sci*, 9 (2014) 2341.
21. J.C. Claussen, A. Kumar, D.B. Jaroch, M.H. Khawaja, A.B. Hibbard, D.M. Porterfield and T.S. Fisher, *Adv Funct Mater*, 22 (2012) 3399.
22. M. Pumera, A. Ambrosi, A. Bonanni, E.L.K. Chng and H.L. Poh, *TrAC-Trend Anal Chem*, 29 (2010) 954.
23. C. Bergemann, D. Müller-Schulte, J. Oster, L. à Brassard and A.S. Lübbe, *J Magn Magn Mater*, 194 (1999) 45.
24. A.-H. Lu, E.L. Salabas and F. Schüth, *Angew Chem Int Edit*, 46 (2007) 1222.
25. L. Gao, J. Zhuang, L. Nie, J. Zhang, Y. Zhang, N. Gu, T. Wang, J. Feng, D. Yang, S. Perrett and X. Yan, *Nat Nano*, 2 (2007) 577.
26. P.K. Srivastava, A.M. Kayastha and Srinivasan, *Biotechnol Appl Biochem*, 34 (2001) 55.
27. S. Sungur, M. Elcin and U. Akbulut, *Biomaterials*, 13 (1992) 795.
28. S.M. Naghib, M. Rabiee and E. Omidinia, *Int. J. Electrochem. Sci*, 9 (2014) 2301.
29. E. Omidinia, S.M. Naghib, A. Boughdachi, P. Khoshkenar and D.K. Mills, *Int. J. Electrochem. Sci*, 10 (2015) 6833.
30. S.M. Naghib, *Anal. bioanal. electrochem*., 8 (2016) 453.
31. P. Moozarm Nia, W.P. Meng, F. Lorestani, M.R. Mahmoudian and Y. Alias, *Sensor Actuat B-Chem*, 209 (2015) 100.
32. L.-M. Lu, H.-B. Li, F. Qu, X.-B. Zhang, G.-L. Shen and R.-Q. Yu, *Biosens Bioelectron*, 26 (2011) 3500.
33. J. Luo, S. Jiang, H. Zhang, J. Jiang and X. Liu, *Anal Chim Acta*, 709 (2012) 47.
34. H. Yu, X. Jian, J. Jin, X.-c. Zheng, R.-t. Liu and G.-c. Qi, *Microchim Acta*, 182 (2015) 157.
35. X. Cao and N. Wang, *Analyst*, 136 (2011) 4241.
36. S.K. Meher and G.R. Rao, *Nanoscale*, 5 (2013) 2089.
37. F. Meng, W. Shi, Y. Sun, X. Zhu, G. Wu, C. Ruan, X. Liu and D. Ge, *Biosens Bioelectron*, 42 (2013) 141.
38. X. Zhang, A. Gu, G. Wang, Y. Huang, H. Ji and B. Fang, *Analyst*, 136 (2011) 5175.
39. Y. Zhang, Y. Wang, J. Jia and J. Wang, *Sensor Actuat B-Chem*, 171 (2012) 580.
40. B. Yuan, C. Xu, L. Liu, Q. Zhang, S. Ji, L. Pi, D. Zhang and Q. Huo, *Electrochim Acta*, 104 (2013) 78.
41. S. Cherevko and C.-H. Chung, *Talanta*, 80 (2010) 1371.
42. Y. Mu, D. Jia, Y. He, Y. Miao and H.-L. Wu, *Biosens Bioelectron*, 26 (2011) 2948.
43. X. Kang, Z. Mai, X. Zou, P. Cai and J. Mo, *Anal Biochem*, 363 (2007) 143.
44. J. Wang, D.F. Thomas and A. Chen, *Anal Chem*, 80 (2008) 997.
45. L. Özcan, Y. Şahin and H. Türk, *Biosens Bioelectron*, 24 (2008) 512.
46. M. Liu, R. Liu and W. Chen, *Biosens Bioelectron*, 45 (2013) 206.
47. K.M. El Khatib and R.M. Abdel Hameed, *Biosens Bioelectron*, 26 (2011) 3542.
48. L.-Q. Rong, C. Yang, Q.-Y. Qian and X.-H. Xia, *Talanta*, 72 (2007) 819.

49. L. Zhang, H. Li, Y. Ni, J. Li, K. Liao and G. Zhao, *Electrochem Commun*, 11 (2009) 812.
50. X. Wang, Y. Zhang, C.E. Banks, Q. Chen and X. Ji, *Colloid Surface B*, 78 (2010) 363.
51. C. Xia and W. Ning, *Electrochem Commun*, 12 (2010) 1581.